Accepted Manuscript

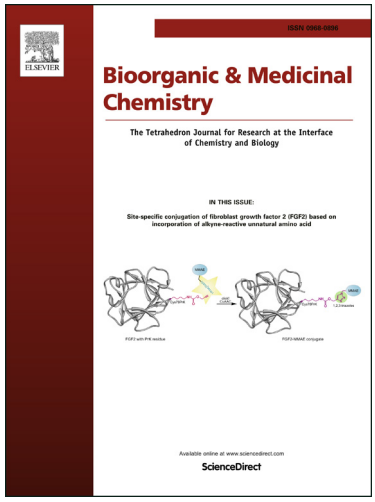

Synthesis of novel flavonoid alkaloids as α-glucosidase inhibitors

Jing Zhen, Yujie Dai, Tom Villani, Daniel Giurleo, James Simon, Qingli Wu

PII: S0968-0896(17)30874-X
DOI: http://dx.doi.org/10.1016/j.bmc.2017.07.055
Reference: BMC 13892

To appear in: *Bioorganic & Medicinal Chemistry*

Received Date: 22 May 2017
Revised Date: 27 July 2017
Accepted Date: 28 July 2017

Please cite this article as: Zhen, J., Dai, Y., Villani, T., Giurleo, D., Simon, J., Wu, Q., Synthesis of novel flavonoid alkaloids as α-glucosidase inhibitors, *Bioorganic & Medicinal Chemistry* (2017), doi: http://dx.doi.org/10.1016/j.bmc.2017.07.055

Synthesis of novel flavonoid alkaloids as α-glucosidase inhibitors

Jing Zhen[1,2], Yujie Dai[3], Tom Villani[1,2], Daniel Giurleo[1,2], James Simon[1,2 *], Qingli Wu[1,2 *]

[1] The New Use Agriculture and Natural Plant Products Program, Department of Plant Biology, Rutgers University, 59 Dudley Road, New Brunswick, NJ 08901, USA

[2] Department of Medicinal Chemistry, Ernest Mario School of Pharmacy, Rutgers University, 160 Frelinghuysen Road, Piscataway, NJ 08854, USA

[3] Key Laboratory of Industrial Fermentation Microbiology, Tianjin University of Science and Technology, Tianjin 300457, China

*Correspondence authors

Qingli Wu, email: qlwu@sebs.rutgers.edu; Tel: +1 848-932-6238

James E Simon, email: jimsimon@rutgers.edu; Tel: +1 848-932-6239

Address: Department of Plant Biology, Rutgers University, 59 Dudley Road, New Brunswick, NJ 08901, USA

Abstract

A series of novel flavonoid alkaloids were synthesized with different flavonoids and attached nitrogen-containing moieties. These new compounds were screened for inhibitory activity of α-glucosidase, among which compound **23** was found to show the lowest IC_{50} of 4.13 μM. Kinetic analysis indicates that the synthesized compounds **15** and **23** inhibit the enzyme in a non-competitive model with *Ki* value of 37.8 ± 0.8 μM and 13.2 ± 0.6 μM. Further docking studies suggest that the preferred binding pocket is close to the catalytic center, correlating to the experimental results. Structure activity relationship studies (SAR) indicate that 4'-hyroxyl group and the 4-position carbonyl group in the flavonoid structure are important for this biological activity. Addition of extra hydrogen bonding and hydrophobic groups on ring A would increase the inhibitory activity.

Keywords: Flavonoid alkaloid; Flavonoid; α-Glucosidase inhibitor; Diabetes; Molecular docking study; SAR

1. Introduction

Diabetes is one of the most common chronic diseases with estimated 387 million patients worldwide and responsible for 4.9 million deaths in 2014 [1]. The number of diabetes patients is projected to rise to more than 592 million in 2035 [2]. Diabetes is a group of metabolic diseases characterized by high blood glucose levels. One of the important therapeutic approaches is to inhibit digesting enzymes such as α-glucosidase, or α-amylase in the intestine to slow down the digestion and absorption of the sugar and to suppress post-prandial hyperglycemia [3]. *α*-Glucosidase hydrolyzes the 1-4 linked *α*-glucose residue from the non-reducing side to release a single α-glucose, acting as the final step in the digestion of dietary carbohydrates. This enzyme α-glucosidase has also been associated with other diseases such as cancer and viral infection [4, 5]. Its inhibitors, such as acarbose, miglitol and voglibose, which are carbohydrate mimetics or derivatives, have already been marketed for the treatment of Type II diabetes mellitus [6]. These drug molecules can decrease both postprandial hyperglycaemia and hyperinsulinaemia, yet also have gastrointestinal adverse effects including diarrhea, flatulence and abdominal discomfort, which limit a long-term compliance to therapy [7]. Developing more efficient and safer inhibitors for hyperglycemia control in diabetes remains a global heath priority.

With the exception of carbohydrate mimetic inhibitors, flavonoid compounds such as luteolin, naringenin, also have been reported to act as potential glucosidase inhibitors that provide protective effects in diabetes therapy both *in vitro* and *in vivo*. [8, 9]. However, their clinical applications for the treatment of diabetes are usually limited by their low solubility and the lack of selectivity. The introduction of nitrogen moieties may increase

the solubility of parent flavonoid compounds, because of its formation of salt with the addition of acids, such as hydrochloric or trifluoroacetic acid [10]. Structure modifications on flavonoid compounds could then further increase their selectivity and efficacy toward specific targets. For example, the introduction of phenylethenyl group at the position 6 of naringenin greatly increases its inhibition toward cyclooxygenase-1 (COX-1) and shows much improved anticancer activity *in vitro* and *in vivo* (Figure 1) [11]. The flavonoid derivatives containing a nitrogen moiety are referred to as flavonoid alkaloids. and have for decades been reported to exhibit various biological activities including anticancer, anti-virus, anti-inflammation and others [12]. The introduction of a nitrogen moiety to the flavonoid,, such as with flavopiridol (Figure 1), derived from flavonoid, inhibited cyclin-dependent kinases CDK1 and CDK2 and now serves as an anti-cancer drug candidate in clinical trials [13]. The introduction of a nitrogen moiety may also increase the binding affinity with target enzyme and result in lower IC_{50} values with higher therapeutic efficacy. Therefore, in this study, we sought to synthesize novel flavonoid alkaloids that would enhance α-glucosidase inhibitory activities. There are limited studies that have reported on the structure activity relationship between the flavonoid derivatives and α-glucosidase and the related inhibitory mechanism. As such, in this study, we also conducted enzymatic kinetics study and molecular modeling studies on selected representative compounds with high inhibitory activity and further investigated their structure activity relationships, which may help drug molecule design targeting α-glucosidase in the future.

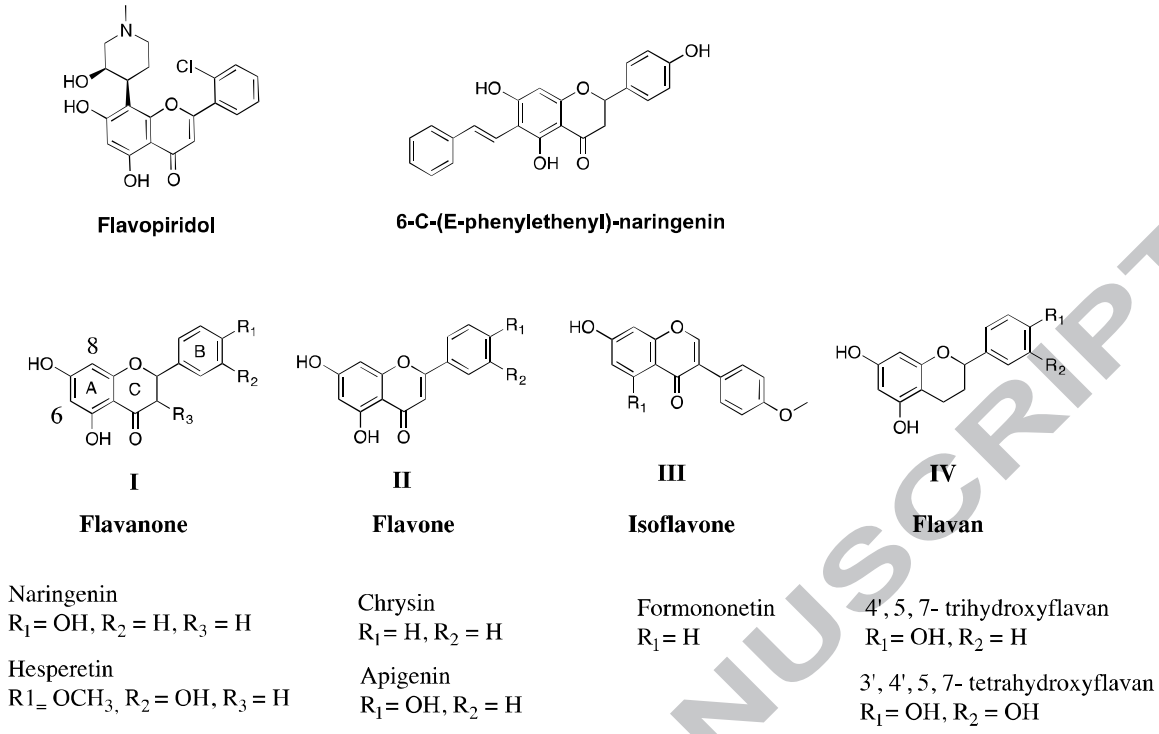

Figure 1. The general structure of flavonoids used for derivative synthesis.

In this study, various nitrogen-containing moieties were attached to the four different members of the flavonoid family, including flavone, flavanone, isoflavone and flavan (Figure 1). The inhibitory activities of synthesized derivatives were tested on α-glucosidase produced from yeast *Saccharomyces cerevisiae*, and the results indicated that compounds **15** and **23** showed the best inhibitory activity with IC_{50} value of 23.43 and 4.13 μM, respectively. Their inhibitory kinetics and mechanism were explored with various concentrations of compounds and substrates. The data analysis was conducted using Lineweaver–Burk and Dixon plots. Results indicated that compounds **15** and **23** inhibit the enzyme in a non-competitive manner with *Ki* value of 37.8 ± 0.8 and 13.2 ± 0.6 μM, respectively. Molecular docking studies performed on Autodock vina showed the chirality at position 2 has limited effect on the binding affinity and docking positions. In

the docking study, three locations were identified as the potential binding sites on the surface of α-glucosidase. Among these three docking sites, the one with highest binding affinity (location A in Figure **5**) correlates very well with both the literatures and our experimental data in terms of its non-competitive binding mechanism [14]. Binding mechanism analysis at location A indicates that there are hydrogen bonds and hydrophobic interactions between synthesized compounds and surrounding amino acid residue. The aim of this study is to improve the inhibitory activities of flavonoid alkaloids and explore their inhibitory mechanism, both of which would potentially help for the future drug development targeting α-glucosidase for the treatment of diabetes.

2. Results and Discussion

2.1. Chemistry

For the synthesis of flavonoid alkaloids **1-8**, cyclic imine Δ^1-piperideines (1.25 eq), was added into the flavonoids in solvent methanol and then the mixture was stirred at 80 °C for overnight. For flavonoid alkaloids **9-23**, a 37% formaldehyde solution (1.25 eq) and the corresponding secondary amine (1.25 eq) was added into the flavonoid methanol solution. The mixture was then stirred and heated for hours until reaction was completed. TLC was used to monitor the completion of reactions. Afterward, the solvent of each reaction was separately removed and the residue was applied on silica gel chromatography for purification using various solvent systems. Due to the very close chemical properties between positions 6 and 8 of the flavonoid precursors, the site of alkylation under Mannich reaction varies depending on the solvent, temperature, and reaction time (Figure 2A). Flavonoids with different chemical properties have distinct

regioselectivity toward electrophilic substitution. Chen et al.,reported that if the reaction is well performed under mild conditions with limited hours, high regioselectivity toward the position 6 of naringenin was obtained [15]. Nguyen et al. reported that the use of solvent system H_2O /THF (2:1) at 40 °C would yield 99:1 selectivity between positions 6 and 8 [16]. The addition of a base may reverse the reaction and change the ratio of formed products. Low yield was observed, as compounds **1-8**, with the presence of secondary amine functional group, are very likely to be absorbed on silica gel column during purification. For the synthesized compounds presented in this study, the structure of each compound was fully elucidated based on ^{1}H NMR, ^{13}C NMR and 2D NMR. Substitution at positions 6 or 8 was determined based on published literature and/or the proton NMR signals. For example, flavonoid chrysin has proton NMR peaks at 6.17 ppm for H-6 and 6.40 ppm for H-8, in which H-6 is closer to the high field than H-8 with about 0.2 ppm in DMSO-d_6. In the ^{1}H-NMR spectra of synthesized derivatives, for example, the H-6 signal (5.78 ppm) of compound **5** is still around ~ 0.2 ppm closer to the high field than the H-8 peak (5.98 ppm) of compound **4**. This phenomenon was further confirmed in our study by HMBC. It was observed there is correlation between H-6 between C-5, C-7 in compound **4** (Figure 2B).

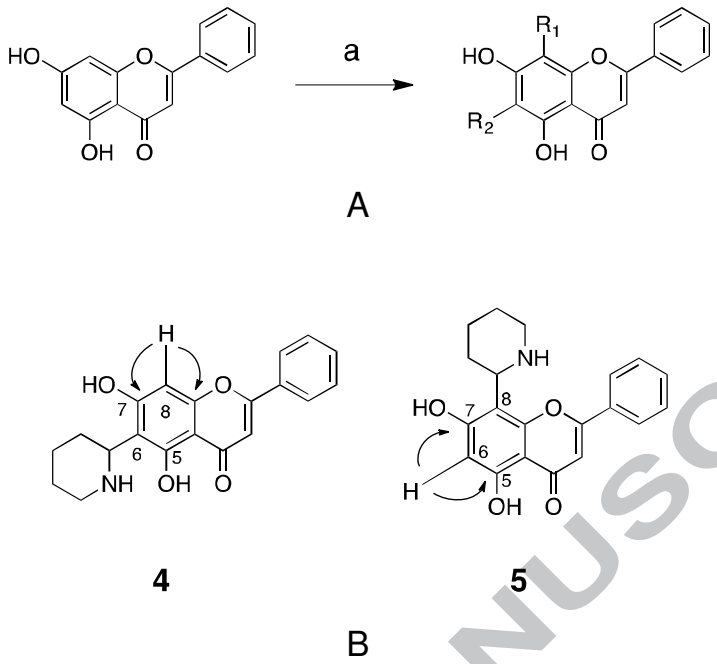

Figure 2. Representative synthetic route of flavonoid alkaloids (A): (a) Δ^1-piperideines, methanol/THF, 80 °C (**1-8**) or secondary amine, 37% HCHO, methanol (**9-23**). Structures of isomers **4, 5** and their HMBC correlation (B).

2.2 Biological activity

All synthesized compounds were screened against α-glucosidase enzyme from yeast along with flavonoid compound naringenin, which is a known α-glucosidase inhibitor and used as a positive control. In this study, the measured IC_{50} of naringenin is 77 μ M and correlates well to the value reported [9]. The concentration of compounds measured against α-glucosidase range from 3.15 to 806 μM. Some compounds start from relatively poor concentrations due to the lower solubility. The inhibitory potency of each compound was evaluated by its IC_{50} value, which was computed out from the fitting to a sigmoidal dose-response curve with variable slope. At least three independent experiments were performed to determine the IC50 values for each compound. Their IC_{50} values, the

indicator of the inhibition strength against α-glucosidase, are summarized in Table **1**. Among these screened compounds, **9**, **15**, **20** and **23** exhibited strong inhibition against α-glucosidase with IC_{50} values of 82.76, 23.43, 65.11 and 4.13 μM, respectively. Their dose-response curves are shown in Figure **3**.

Table 1. Synthesized flavonoid alkaloids and their inhibitory activities

NO.	Flavonoid Moiety	Alkaloid Moiety	Position	Substituted Groups			Inhibitory activity (IC_{50} in μM)
				R_1	R_2	R_3	
1	I		6	OH	H	H	249.4
2			6	OCH_3	OH	H	> 500
3			6	OH	OH	OH	> 500
4	II		6	H	H	-	> 500
5			8				> 500
6	I		6	OH	H	H	293.3
7	IV		6	-	-	-	> 500
8			8	-	-	-	> 500
9	I		6	OH	H	H	82.8
10	II		6	H	H	-	> 500
11	III		8	H	-	-	> 500
12	II		6	H	H	-	217.0
13	I		6	OH	H	H	202.5
14	II		6	H	H	-	> 500
15	I	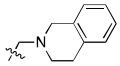	6	OH	H	H	23.4
16	II		6	H	H	-	> 500
17	I	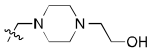	6	OH	H	H	521.0
18	II		6	H	H	-	> 500
19			8				> 500
20	I	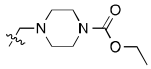	6	OH	H	H	65.1
21	II		6	H	H	-	> 500
22			6 & 8	H	H	-	> 500
23	I	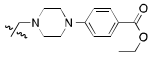	6	OH	H	H	4.1

*Note: The general structure of flavonoid moiety is included in Figure **1**.*

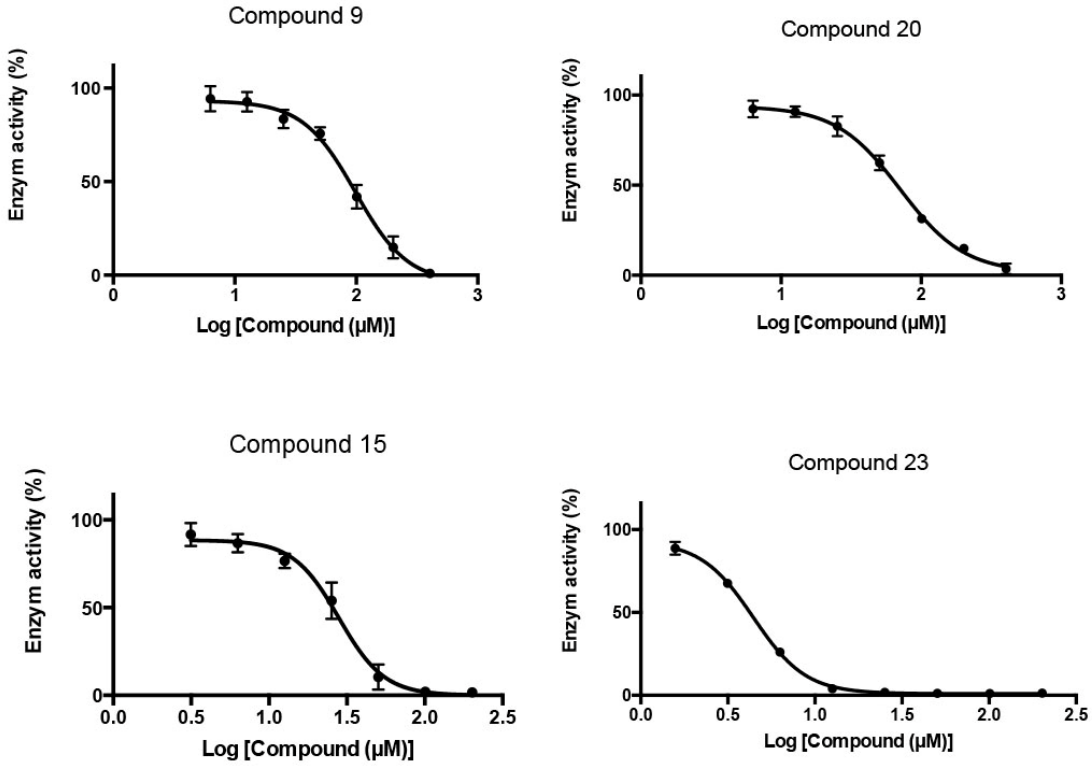

Figure 3. α-Glucosidase inhibitory activity of compounds **9**, **15**, **20** and **23.**

The enzyme kinetic assays were performed on compounds **15** and **23** to investigate their mode of inhibition toward α-glucosidase. In the kinetic studies, a range of concentrations of test compounds and substrates were used. The data was analyzed using Lineweaver-Burk and Dixon plots (Figure **4**) [17]. The Lineweaver-Burk plot was drawn by plotting inverse velocity (*1/V*) as a function of the inverse substrate concentration (*1/[S]*), while the Dixon plot was created by plotting inverse velocity (*1/V*) as a function of the compound concentration (*[I]*). Results showed that both compound **15** and **23** are very close to the non-competitive model inhibitor against α-glucosidase. Their K_i value shown from Dixon plot, are 37.8 ± 0.8 and 13.2 ± 0.6 μM, respectively.

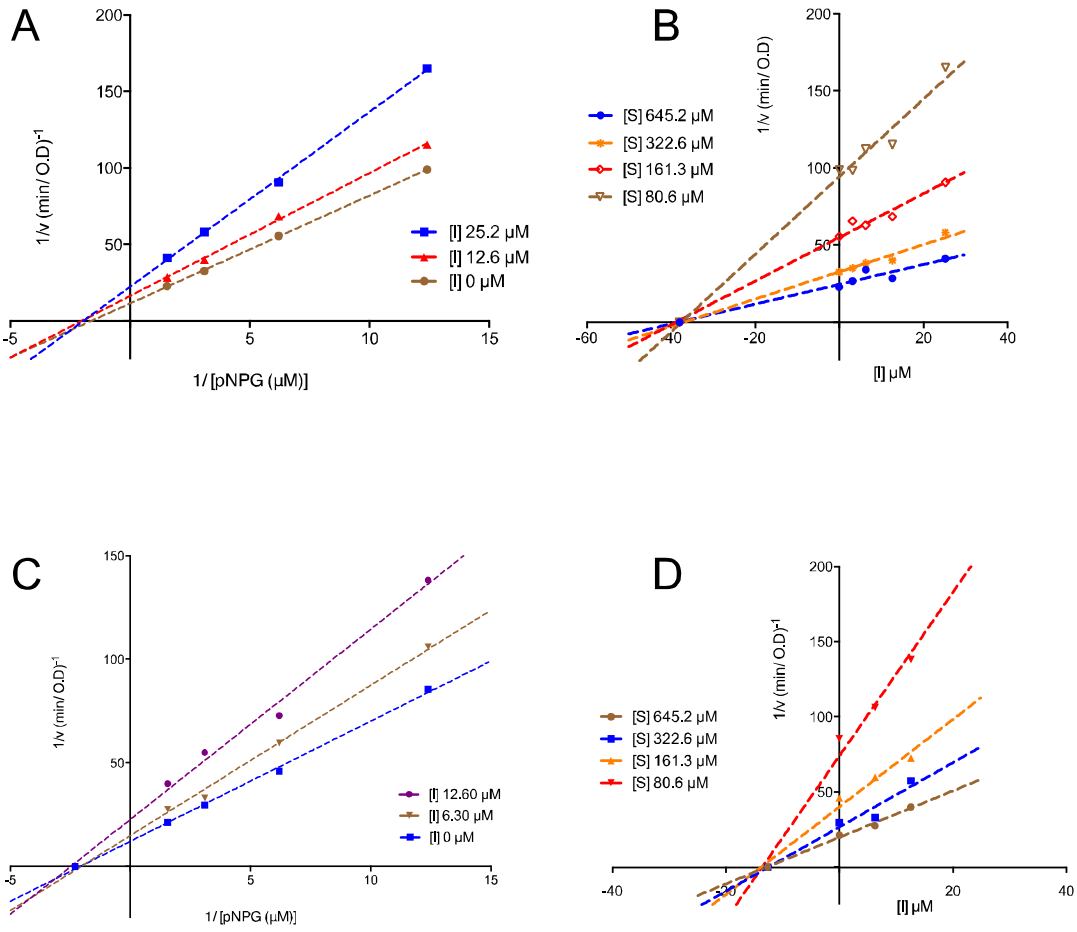

Figure 4. Lineweaver-Burk and Dixon plots of compounds **15** and **23** toward the inhibition of α-glucosidase. Lineweaver-Burk plot of compound **15** (A); Dixon plot of compound **15** (B); Lineweaver-Burk plot of compound **23** (C); Dixon plot of compound **23** (D).

2.3 Molecular Modeling

To envisage the binding model between synthesized inhibitor and α-glucosidase, a molecular docking study was performed. After geometric optimization, both enantiomers of compounds **15** and **23** were docked into the entire protein molecule. There are mainly three different docking sites, in which site A has the best correlation with non-competitive features and highest binding affinity [14]. The other two positions B and C

have comparatively less binding affinity and are very close to the glucose ligand binding pocket, contradicting the non-competitive mode. From the preliminary docking results, it was observed that the R or S isomers share almost the same binding sites on the protein through random screening. Their positions are very close when bound with the protein at the binding site A, suggesting the chirality at position 2 has limited impact on docking results. Even if site A is not directly responsible for the hydrolysis of carbohydrates, after binding with small molecules, it could alter protein conformation and interfere indirectly with the catalytic function (Figure **5**). Secondary docking was performed on site A within smaller area and yielded refined results for binding analysis. The binding site A close to the catalytic center is formed by amino acid residues ARG 263, ARG 270, HIS 195, GLY 169, ASN 259, TRP 15, LYS 16, LEU 297, SER 298, TRP 343 (Figure **6**). There are two arginine amino acids, ARG 263, ARG 270 at the entrance of the pocket, which are positively charged at experimental pH 6.8 and may interact with the 4'-hydroxyl group on flavonoid ring C. The hydrophobic pocket end, formed by two tryptophan amino acids TRP 15 and TRP 343, is likely to interact with the hydrophobic groups, such as the tetrahydroisoquinoline group of compound **15** and the ethyl benzoate group of compound **23**. Three hydrogen bonds were observed for compound **15**: the carbonyl group of position 4 and the amine on the imidazole of HIS 295 (2.67 Å), phenol group at position 5 and the carbonyl group of ASN 259 (3.08 Å), phenol group at position 7 and the carboxylic acid group of SER 298 (2.79 Å). For compound **23**, there are two hydrogen bonds: phenol of position 7 and the amine moiety of HIS 195 (3.20 Å), the carbonyl group of ester group on alkaloid moiety and the amine moiety of LYS 16 (3.02 Å).

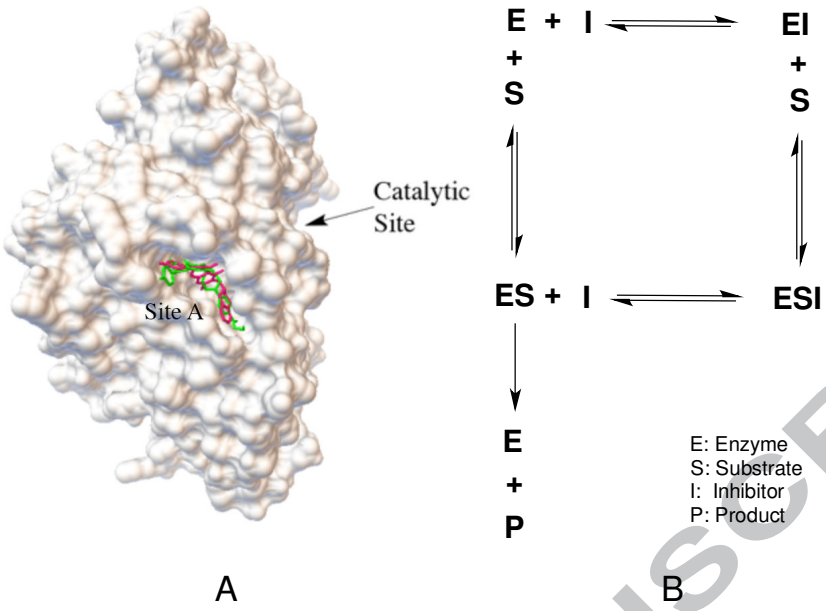

Figure 5. The discovered binding site A between synthesized compounds **15**, **23** and α-glucosidase (A); the scheme of non-competitive inhibition (B).

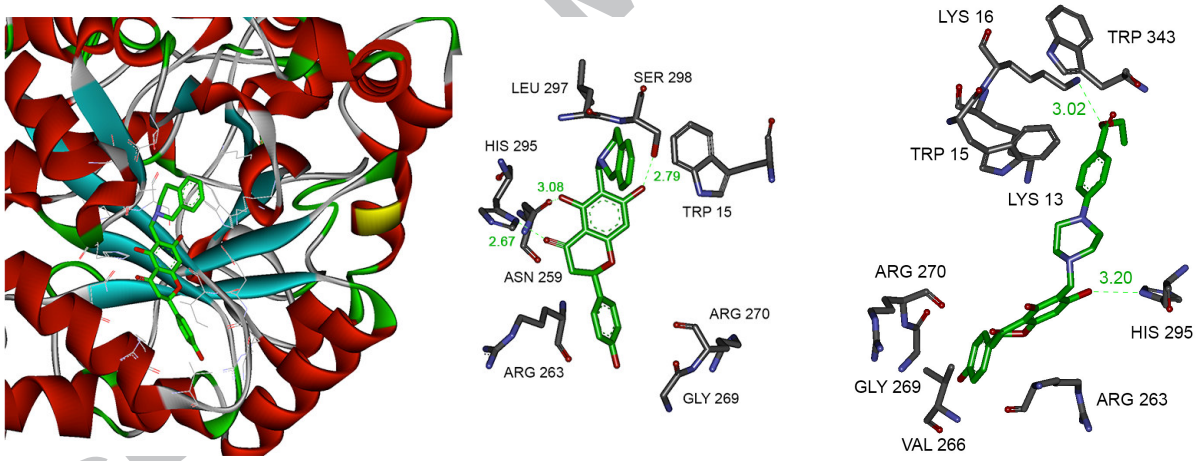

Figure 6. The binding model between compounds **15** and **23** and α-glucosidase at binding site A.

2.4 Structure Activity Relationship

In this study, most of the analogues are synthesized from the flavanone naringenin and the flavone chrysin. Comparing compounds 1 and 2 to that of compounds 4 and 6, it was expected to find that the hydroxyl group attached at ring position 4' on ring B is very essential for inhibitory activity. However, excessive hydroxyl groups at position 3 and 3' could also decrease inhibitory affinity, as suggested by compound 3. The importance of 4'-hydroxyl group was also suggested by the docking results, in which there may be an interaction with positively charged arginine groups (ARG 263, ARG 270) at the entrance of the binding pocket. Most chrysin derivatives without 4'-hydroxyl group have no inhibitory activities. The flavan derivatives didn't show activities less than 500 μM, underlying the importance of C=O at position 4. Further study on more flavan derivatives are needed to confirm this observation. The introduction of tertiary amine appears to provide improved inhibitory activity than the secondary amine group as suggested from the comparison between compound **1** and compound **9**. Attachment of hydrophobic groups at flavonoid ring A yields better activity as compound **15** is more potent than **18**; **23** is more potent than **21**. The addition of an extra hydrogen bond acceptor at the side end of the attached moiety may increase the binding with α-glucosidase through hydrogen bonding. For example, compound **23** has a hydrogen bonding with LYS 16 through the carbonyl group of ester moiety. The proposed structure activity relationships are illustrated in Figure **7**.

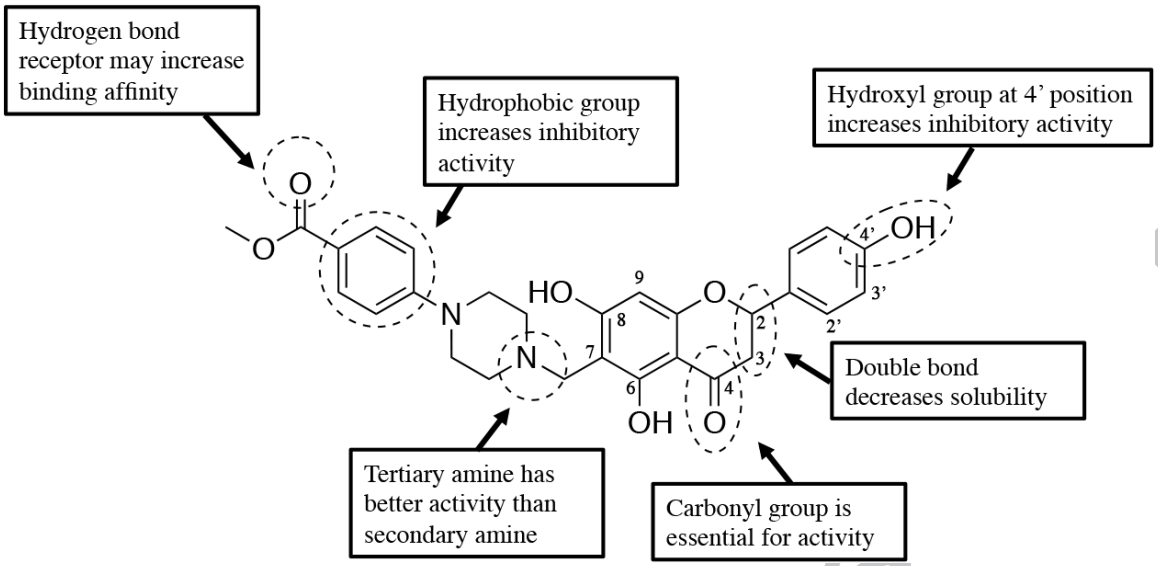

Figure 7. The proposed structure activity relationships

3. Conclusions

In our study, a collection of flavonoid derivatives was synthesized through Mannich reaction targeting for the inhibition of α-glucosidase. Most of the compounds synthesized from flavanone naringenin exhibited potent bioactivities with IC_{50} values below 500 μM, in which the most potent compound **23** has IC_{50} value of 4.13 μM. Enzyme kinetic investigation suggests the synthesized compounds inhibit enzyme in the non-competitive manner with *Ki* value of 37.8 ± 0.8 and 13.2 ± 0.6 μM for compound **15** and **23**, respectively. The molecular docking study suggested synthesized derivatives might bind to a pocket close the catalytic center and interfere the catalysis process indirectly. The binding model between α-glucosidase and compounds at location A were carefully analyzed, in which several hydrogen bonds and hydrophobic interactions were revealed. Based on tested activities of compounds and SAR, it was found that the hydroxyl group at position 4' is essential to exhibit biological activity, and that the introduction of

hydrophobic groups and hydrogen acceptors at flavonoid ring A would potentially increase the binding affinity and yield higher inhibitory activity.

4. Experimental

4.1. General

^{1}H and ^{13}C NMR spectra were performed on Bruker Avance 400 MHz spectrometer (Billerica, MA). Analytical LC-MS was performed on Hewlett-Packard Agilent 1100 series HPLC-MSD (Agilent Technologies, Waldbronn, Germany) equipped with a quaternary pump system, a degasser, an auto-sampler, a DAD detector, a MSD trap with electrospray ion source (ESI). Column chromatography was performed using silica gel (230 - 400 mesh; Selecto Scientific, Suwanee, GA). All synthetic materials including the solvents and enzyme *α-glucosidase* are all purchased from Sigma Aldrich (St. Louis, MO).

4.2 In vitro α-glucosidase assay

The assay was performed based on a chromogenic reported method with slight modifications [18]. In brief, 10 µl of enzyme solution (1 U/ml) was diluted with 120 µl of 0.1 M phosphate buffer (pH 6.8). Then 5 µl of the compound solution prepared in DMSO with various concentrations were added into the enzyme solution. The final concentration of DMSO is around 2%. The mixture was then incubated at 37°C for 15 min. Afterward 20 µl of 5 mM substrate p-nitrophenyl- α-D-glucopyranoside in phosphate buffer (pH 6.8) were added and incubated for additional 30 min at 37°C. The reaction was quenched using 80 µl of 0.2 M Na_2CO_3. Absorption was subsequently measured using UV

spectrometer at wavelength of 405 nm. The reaction without enzyme was treated as blank and each experiment was triplicated. The inhibitory activity was calculated using the following equation:

Inhibition % = [(control absorption – sample absorption) / control absorption] × 100 %

The IC_{50} value of each sample was calculated from the fitting of sigmoidal dose-response curve with variable slope.

4.3. Enzymatic kinetics of α-glucosidase inhibition

Mode of inhibition of synthesized flavonoid alkaloids against yeast α-glucosidase activity was measured with different concentrations of pNPG (0.625, 1.25, 2.5, 5.0 mM). Control group has no compound added. Mode of inhibition of each tested compound was determined by Lineweaver-Burk plot analysis. The Dixon plots were applied to determine the inhibitory constants with the following equation, where V is the reaction velocity, S is substrate concentration, V_{max} is the maximum enzyme velocity, K_m is Michaelis-Menten constant, I is inhibitor concentration, K_i is inhibition constant and α is the constant that determines mechanism. In this study, for non-competitive inhibitor, $\alpha = 1$. If α is very large, then the mode approaches a competitive model. If α is very small but greater than zero, the mode is more closer to uncompetitive model [14].

$$V = \frac{Vm\,S}{Km\left(1 + \frac{I}{Ki}\right) + S\,(1 + \frac{I}{\alpha Ki})}$$

4.4. Molecular Docking

Molecular docking has been commonly used in medicinal chemistry research [19]. The crystallographic structure of -glucosidase (PDB: 3A4A) was downloaded from the Protein Data Bank (http://www.rcsb.org/pdb/). All polar hydrogen atoms and charges were assigned to the receptor using AutoDockTools 1.5.4. Compounds used for docking study were built using the molecular builder function in MOE 2010.11 (http://www.chemcomp.com/), the energy of each compound was minimized to its local minima using MMF94X force field to a constant value of 0.05 kcal/mol. Docking simulation and binding pocket prediction was performed using AutoDock Vina (http://vina.scripps.edu/) [20]. The protein was held rigid in the docking process. The inhibitors were allowed to flexible. The initial grid box size was 62 Å× 78 Å×1 72Å in the x, y, z dimensions. The grid box center was put on x = 23.8, y = -3.834 and z = 19.691 with the protein positioned at the center of the box. The docking method would be validated using its competitive inhibitor acarbose and glucosidase. The resulting docked poses were analyzed with AutoDockTools using cluster analysis, PyMOL (https://www.pymol.org) [21]. Using the established method, control compound acarbose was docked into the catalytic binding pocket, which correlates well with published literature [22] and its competitive inhibition mechanism against α-glucosidase.

4.5. Chemical synthesis

*4.5.1 General procedure for synthesis of compound **1-8***

The flavonoid compound (1 mmol, 1.0 eq) was dissolved in methanol or methanol/ tetrahydrofuran followed by the addition of Δ^1-piperideines (124 mg, 1.25 mmol, 1.25 eq). The mixture was then stirred at 80 °C under nitrogen atmosphere for 5 hours. After

the reaction, the solvent was removed under reduced pressure and the residue was purified on silica gel column using dichloromethane/ methanol in gradient to obtain the desired compound.

*4.5.1.1 5, 7-dihydroxy-2-(4-hydroxyphenyl)-6-(piperidin-2-yl)chroman-4-one (**1**)*

Yield: 78 %. White powder. ESI-MS: *m/z* 356 $[M+H]^+$, ^{1}H NMR (400 MHz, DMSO-d_6): δ 1.50-1.90 (6H, m, H- 4'', 5'', 6''), 2.47 (1H, m, H-3), 2.75 (1H, m, H-3''), 2.98 (1H, m, H-3), 3.29 (1H, m, H-3''), 4.16 (1H, m, H-1''), 5.20 (1H, m, H-2), 5.33 (1H, s, H-8), 6.78 (2H, H-3', 5'), 7.28 (2H, H-2', 6'); ^{13}C NMR (100 MHz, DMSO-d_6): δ 22.44, 22.54 (C-4'', 5''), 28.15 (C-6''), 41.86 (C-3), 43.52 (C-3''), 52.05 (C-1''), 77.48 (C-2), 96.91 (C-10), 98.01 (C-8), 104.58 (C-6), 115.05 (C-2', 6'), 128.01 (C-3', 5'), 129.75 (C-1'), 157.40, 160.01, 161.56, 177.67 (C-4', 5, 7, 9), 191.51 (C-4, C=O).

*4.5.1.2 5, 7-dihydroxy-2-(3-hydroxy-4-methoxyphenyl)-6-(piperidin-2-yl)chroman-4-one (**2**)*

Yield 60%. White solid. ESI-MS: m/z 386 $[M+H]^+$; ^{1}H NMR (400 MHz, DMSO-d_6): δ 1.50-1.90 (6H, m, H- 4'', 5'', 6''), 2.54 (1H, m, H-3), 3.27 (1H, m, H-3''), 2.92 (1H, m, H-3), 3.27 (1H, m, H-3''), 3.76 (1H, s, -OCH_3), 4.16 (1H, m, H-1''), 5.18 (1H, m, H-2), 5.35 (1H, s, H-8), 6.84 (2H, H-5'), 6.91 (2H, H-2', 6'); ^{13}C NMR (100 MHz, DMSO-d_6): δ 22.45, 22.54 (C-4'', 5''), 28.2 (C-6''), 41.9 (C-3), 43.5 (C-3''), 52.0 (C-1''), 55.7 (-OCH_3), 77.3 (C-2), 96.9 (C-8), 98.5 (C-10), 104.6 (C-6), 112.0 (C-5'), 113.9 (C-2'), 117.3 (C-6'), 132.1 (C-1'), 146.5, 147.6 (C-3', 4'), 161.5, 160.0, 177.7 (C-5, 7, 9), 191.4 (C-4, C=O).

*4.5.1.3 2-(3, 4-dihydroxyphenyl)-3, 5, 7-trihydroxy-6-(piperidin-2-yl)chroman-4-one (**3**)*

Yield: 25 %. Yellow solid. ESI-MS: *m/z* 388 $[M+H]^+$; ^{1}H NMR (400 MHz, DMSO-d_6) (mixture of isomers): δ 1.53-1.70 (6H, m, H-4'', 5'', 6''), 2.79 (1H, m, H-3''), 3.30 (1H, m, H-3''), 4.21 (1H, m, H-1''), 4.27 (1H, d, J = 10 Hz, H-3), 4.75 (1H, d, J = 10 Hz, H-2), 5.40 (1H, s, H-8), 6.84 (1H, m, H-5'), 6.70 (2H, m, H-2', 6'); ^{13}C NMR (100 MHz, DMSO-d_6): δ 22.41, 27.80, 29.48 (C-4'', 5'', 6''), 43.78 (C-3''), 51.90 (C-1''), 82.42 (C-2), 104.59 (C-6), 97.80 (C-10), 95.95 (C-8), 119.10 (C-2', 6'), 115.10 (C-5'), 145.51, 160.78 (C-3', C-4'), 159.98, 161.43 (C-5, 9), 161.32 (C-7), 192.6 (C-4).

*4.5.1.4 5,7-dihydroxy-2-phenyl-6-(piperidin-2-yl)-4H-chromen-4-one (**4**)*

Yield: 26 % (together with 14% compound **5**). Pale yellow solid. ESI-MS: *m/z* 338 $[M+H]^+$; ^{1}H NMR (400 MHz, DMSO-d_6): δ 1.55-1.85 (6H, m, H-4'', 5'', 6''), 2.75 (1H, m, H-3''), 3.31 (1H, m, H-3''), 4.26 (1H, m, H-1''), 5.98 (1H, s, H-8), 6.71 (1H, s, H-3), 7.55 (3H, m, H-3', 4', 5'), 7.99 (2H, m, H-2', 6'); ^{13}C NMR (100 MHz, DMSO-d_6): δ 22.52, 22.80, 28.12 (C-4'', 5'', 6''), 43.49 (C-3''), 52.01 (C-1''), 95.90 (C-8), 99.34 (C-10), 108.67 (C-8), 125.00 (C-2', 6'), 130.00 (C-3', 5'), 131.37 (C-4'), 157.46, 157.28, 161.26 (C-5, 9, 2), 173.88 (C-7), 180.14 (C-4).

*4.5.1.5 5, 7-dihydroxy-2-phenyl-8-(piperidin-2-yl)-4H-chromen-4-one (**5**)*

Yield: 14 % (together with 26% compound **4**). Yellow solid. ESI-MS: *m/z* 338 $[M+H]^+$; ^{1}H NMR (400 MHz, DMSO-d_6): δ 1.55-1.83 (6H, m, H-4'', 5'', 6''), 2.89 (1H, m, H-3''), 3.31 (1H, m, H-3''), 4.48 (1H, m, H-1''), 5.78 (1H, s, H-6), 6.78 (1H, s, H-3), 7.59 (3H, m, H-3', 4', 5'), 8.00 (2H, m, H-2', 6'); ^{13}C NMR (100 MHz, DMSO-d_6): δ 22.77, 22.98, 28.93 (C-4'', 5'', 6''), 43.58 (C-3''), 52.69 (C-1''), 101.57 (C-6), 103.77 (C-10), 104.70

(C-8), 125.95 (C-2', 6'), 129.20 (C-3', 5'), 131.48 (C-4'), 153.63, 160.67, 161.05 (C-5, 9, 2), 173.14 (C-7), 180.27 (C-4).

*4.5.1.6 5, 7-dihydroxy-2-(4-hydroxyphenyl)-6-(piperidin-2-yl)-4H-chromen-4-one (**6**)*

Yield: 38 %. Yellow solid. ESI-MS: *m/z* 354 $[M+H]^+$; ^{1}H NMR (400 MHz, DMSO-d_6): δ 1.53-1.78 (6H, m, H-4'', 5'', 6''), 2.80 (1H, m, H-3''), 3.30 (1H, m, H-3''), 4.25 (1H, m, H-1''), 6.07 (1H, s, H-8), 6.58 (1H, s, H-3), 6.89 (2H, m, H-3', 5'), 7.83 (2H, m, H-2', 6'); ^{13}C NMR (100 MHz, DMSO-d_6): δ 22.61, 22.86, 28.21 (C-4'', 5'', 6''), 43.80 (C-3''), 51.95 (C-1''), 102.11 (C-6), 99.74 (C-10), 95.45 (C-8), 127.98 (C-2', 6'), 115.86 (C-3', 5'), 160.78 (C-4'), 157.43, 157.16, 162.28 (C-5, 9, 2), 171.87 (C-7), 180.56 (C-4).

*4.5.1.7 2-(4-hydroxyphenyl)-6-(piperidin-2-yl)chromane-5, 7-diol (**7**)*

Yield: 25 %. White solid. Compounds 7, 8 would be gradually oxidized to purple compounds when exposed to the air. ^{1}H NMR (400 MHz, DMSO-d_6): δ 1.60 (2H, m, H-5'' and H-4''), 1.88 (4H, m, H-3, 4'', 5'', 6''), 2.09 (2H m, H-3, 6''), 2.62 (2H, m, H-4), 2.90 (1H, m, H-3''), 3.30 (1H, d, H-3''), 4.42 (1H, m, H-1''), 4.88 (1H, m, H-2), 6.03 (1H, d, H-8), 6.80 (2H, d, H-2', 6'), 7.20 (2H, d, H-3', 5'); ^{13}C NMR (100 MHz, DMSO-d_6) δ 19.58 (C-4), 21.8, 22.75 (C-4'', 5'') 28.56 (C-6''), 28.54 (C-3), 45.40 (C-3'') 57.65 (C-1''), 76.30 (C-2), 95.35 (C-6), 101.78 (C-10), 104.85 (C-8), 114.98 (C-2', 6'), 127.20 (C-3', 5'), 157.50, 155.53, 154.10, 153.90 (C-5, 7, 9, 4').

*4.5.1.8 2-(4-hydroxyphenyl)-8-(piperidin-2-yl)chromane-5, 7-diol (**8**)*

Yield: 25 %. White solid. ^{1}H NMR (400 MHz, DMSO-d_6): δ 1.60 (2H, m, H-5'' and H-4''), 1.88 (4H, m, H-3, 4'', 5'', 6''), 2.09 (2H m, H-3, 6''), 2.62 (2H, m, H-4), 2.90 (1H,

m, H-3''), 3.00 (1H, m, N-H), 4.32 (1H, m, H-1''), 5.00 (1H, m, H-2), 6.25 (1H, d, H-6), 6.80 (2H, d, H-2', 6'), 7.20 (2H, d, H-3', 5'), ^{13}C NMR (100 MHz, DMSO-d_6) δ 19.58 (C-4), 21.8, 22.75 (C-4'', 5'') 28.56 (C-6''), 28.54 (C-3), 45.40 (C-3'') 57.65 (C-1''), 76.30 (C-2), 95.35 (C-6), 101.78 (C-10), 104.80 (C-6), 114.98 (C-2', 6'), 127.20 (C-3', 5'), 157.50, 155.53, 154.10, 153.90 (C-5, 7, 9, 4').

*4.5.2 General synthetic procedure of compound (**9-23**)*

The flavonoid compound (1.0 mmol, 1.0 eq) was dissolved in methanol followed by the addition of 37% formaldehyde solution (97 µl, 1.2 mmol, 1.2 eq) and the corresponding amine (1.2 mmol, 1.2 eq). The mixture was then stirred at 65°C for various hours. After the reaction, the solvent was removed under reduced pressure and the residue was purified on silica gel column using dichloromethane/ methanol in gradient to obtain the desired compound.

*4.5.2.1 5, 7-dihydroxy-2-(4-hydroxyphenyl)-6-(piperidin-1-ylmethyl)chroman-4-one (**9**)*

Yield: 65 %. Yellow solid. ^{1}H NMR (400 MHz, DMSO-d_6): δ 1.29 (2H, H-5''), 1.40 (4H, H-4'', 6''), 2.44 (1H, H-3, dd, J = 2.8, 17 Hz), 2.49 (4H, H-3'', 7''), 3.01 (1H, H-3, dd, J = 12.6, 17 Hz), 5.17 (1H, H-2, dd, J = 2.8, 12.6 Hz), 5.50 (1H, H-8), 6.62 (2H, H-3', 5'), 7.13 (2H, H-2', 6'); ^{13}C NMR (100 MHz, DMSO-d_6): δ 22.77 (C-5''), 24.50 (C-4'', 6''), 41.83 (C-3), 52.27 (C-1''), 52.32 (C-3'', 7''), 78.07 (C-2), 95.86 (C-8), 99.34 (C-10), 99.80 (C-6), 115.09 (C-3'), 128.20 (C-2'), 129.14 (C-1'), 157.60 (C-4'), 160.99, 161.89, 171.60 (C-9, 5, 7), 194.79 (C-4).

*4.5.2.2 5, 7-dihydroxy-2-phenyl-6-(piperidin-1-ylmethyl)-4H-chromen-4-one (**10**)*

Yield: 21 %. Yellow solid. ^{1}H NMR (400 MHz, DMSO-d_6): δ 1.47 (2H, H-5''), 1.60 (4H, H-4'', 6''), 2.70 (4H, H-3'', 7''), 3.86 (2H, H-1''), 6.41 (1H, H-8), 6.92 (1H, H-2), 7.57-7.59 (3H, H-3', 4', 5'), 8.05 (2H, H-2', 6'); ^{13}C NMR (100 MHz, DMSO-d_6): δ 22.82 (C-5''), 24.55 (C-4'', 6''), 48.54 (C-3'', 7''), 52.51 (C-1''), 94.46 (C-10), 94.85 (C-8), 105.01 (C-6), 105.22 (C-3) 126.26 (C-2', 6'), 129.11 (C-3', 5'), 131.28 (C-4'), 162.04 (C-2), 181.67 (C-4).

*4.5.2.3 7-hydroxy-3-(4-methoxyphenyl)-8-(piperidin-1-ylmethyl)-4H-chromen-4-one (**11**)*

Yield: 51 %. Pale yellow solid. ^{1}H NMR (400 MHz, DMSO-d_6): δ 1.46 (2H, H-5''), 1.57 (4H, H-4'', 6''), 2.58 (4H, H3'', 7''), 3.78 (3H, -OCH_3), 3.90 (2H, H-1'') 6.83 (1H, H-6), 7.0 (2H, H-3', 5'), 7.5 (2H, H-2', 6'), 7.88 (1H, H-5), 8.35 (1H, H-2); ^{13}C NMR (100 MHz, DMSO-d_6): δ 23.24 (C-5''), 25.26 (C-4'', 6''), 52.97 (C-1''), 53.15 (C-3'', 7''), 55.11 (-OCH_3), 107.86 (C-8), 113.67 (C-3', 5'), 115.31 (C-6), 115.92 (C-10), 122.93 (C-1'), 124.22 (C-3), 125.56 (C-5), 130.05 (C-2', 6'), 152.68 (C-2), 155.01 (C-9), 158.92 (C-4'), 163.99 (C-7), 174.64 (C-4).

*4.5.2.4 6-((Diethylamino)methyl)-5,7-dihydroxy-2-phenyl-4H-chromen-4-one (**12**)*

Yield: 45 % (together with 6, 8 di-substituted side product). Yellow solid. ^{1}H NMR (400 MHz, DMSO-d_6): δ 1.27 (3H, -CH_3), 2.61 (4H, H-3'', 7''), 3.5 (4H, H-4'', 6''), 4.01 (2H, H-1''), 4.14 (2H, -OCH_2-), 6.30 (1H, H-8), 6.64 (1H, H-3), 7.53 (3H, H-3', 4', 5'), 7.80 (2H, H-2', 6'); ^{13}C NMR (100 MHz, DMSO-d_6): δ 14.77 (-CH_3), 43.52 (C-4'', 6''), 52.55 (C-1''), 53.97 (C-3'', 7''), 61.82 (-OCH_2-), 98.23 (C-8), 100.45 (C-10), 105.03 (C-3), 106.09 (C-6), 126.21, 129.35, 131.66, 131.96 (C-2', 3', 4', 1'), 154.94 (C-9), 155.36 (-OC=O), 161.94, 163.29, 165.38 (C-2, 5, 7), 182.51 (-C=O).

*4.5.2.5 5, 7-dihydroxy-2-(4-hydroxyphenyl)-6-(morpholinomethyl)chroman-4-one (**13**)*

Yield: 76 %. White solid. ^{1}H NMR (400 MHz, MeOD-d_4): δ 2.59-2.64 (1H, H-3, dd, J = 17.16, 3.1 Hz), 2.72 (4H, H-3'', 7'', m), 2.96- 3.04 (1H, H-3, dd, J = 12.68 17.16 Hz), 3.65-3.68 (4H, H-4'', 5'', m), 3.79 (2H, H-1'', s), 5.21-5.25 (1H, H-2, dd, J = 3.1, 12.68 Hz), 6.71 (2H, H-3', 5', d, J = 8.6 Hz), 7.19 (2H, H-2', 6', d, J = 8.6 Hz), ^{13}C NMR (100 MHz, MeOD-d_4): δ 43.86 (C-3), 52.71 (C-1''), 53.63 (C-3'', 7''), 66.90 (C-4'', 6''), 80.44 (C-2), 96.73 (C-8), 100.79 (C-10), 102.59 (C-6), 116.38, 116.47 (C-3', 5'), 129.02 (C-2' 6'), 131.04 (C-1'), 159.07 (C-4'), 163.43, 164.54 (C-5, 9), 170.07 (C-7), 197.59 (C-4).

*4.5.2.6 5, 7-dihydroxy-6-(morpholinomethyl)-2-phenyl-4H-chromen-4-one (**14**)*

Yield: 46 %. Yellow solid. ^{1}H NMR (400 MHz, DMSO-d_6): δ 2.68 (4H, H-4'', 6''), 3.80 (4H, H-3'', 7''), 4.01 (2H, H-1''), 6.31 (1H, H-8), 6.65 (1H, H-3), 7.56 (3H, m, H-3', 4' 5'), 7.83 (2H, H-2'); ^{13}C NMR (100 MHz, DMSO-d_6): δ 53.02 (C-1''), 54.17 (C-3'', 7''), 66.66 (C-4'', 6''), 98.00 (C-8), 100.31 (C-3), 104.89 (C-10), 105.97 (C-6), 126.11 (C-2'), 129.23 (C-3'), 131.58 (C-4'), 131.82 (C-1'), 154.89 (C-9), 161.80 (C-2), 163.17 (C-5), 165.35 (C-7), 182.40 (C-4).

*4.5.2.7 6-((3, 4-dihydroisoquinolin-2(1H)-yl)methyl)-5,7-dihydroxy-2-(4-hydroxyphenyl) chroman-4-one (**15**)*

Yield: 52 %. White solid. ^{1}H NMR (400 MHz, MeOD-d_4): δ 2.76 (1H, H-3, dd, J = 2.8, 17.2 Hz), 2.97 (4H, -NCH_2CH_2Ar-, br), 3.08 (1H, H-3, dd, J = 12.8, 17.2 Hz), 3.84 (2H, -NCH_2Ar, br), 3.97 (2H, H-1'', s), 5.32 (1H, H-2, dd, J = 2.8, 12.8 Hz), 5.97 (1H, H-8, s),

6.85 (2H, H-2', 6', d, J = 8.8 Hz) 7.00- 7.20 (4H, m, Ar-H), 7.30 (2H, H-3', 5', d, J = 8.8 Hz); ^{13}C NMR (100 MHz, MeOD-d_4): 28.41 (-CH_2-Ar), 43.22 (C-3), 49.96, 52.95, 55.18 (3 × -N-CH_2-), 78.78 (C-1), 96.29 (C-8), 100.22 (C-10), 101.89 (C-6), 115.67 (C-3', 5'), 127.89 (C-2', 6'), 126.19, 126.62, 126.87, 128.74 (4 × Ar-H), 130.43, 132.62, 133.15 (C-2 and 2 × Ar-C), 156.47, 161.30, 162.46 (C-5, 9, 4'), 169.27 (C-7), 195.79 (C-4).

*4.5.2.8 6-((3, 4-dihydroisoquinolin-2(1H)-yl)methyl)-5, 7-dihydroxy-2-phenyl-4H-chromen-4-one (**16**)*

Yield: 12 % (6, 8 di-substituted product formed). Yellow solid. ^{1}H NMR (400 MHz, $CDCl_3$): δ 3.01 (4H, -Ar-CH_2-CH_2-), 3.89, 4.18 (4H, 2 × -N-CH_2-Ar), 6.32 (1H, s, H-8), 6.65 (1H, s, H-2), 7.04-7.19 (4H, m, -Ar-H), 7.50 (3H, m, -Ar-H), 7.85 (2H, m, -Ar-H); ^{13}C NMR (400 MHz, $CDCl_3$): 28.62 (Ar-CH_2-), 50.38, 53.56, 55.90 (3 × -N-CH_2-), 94.95 (C-8), 100.65 (C-10), 105.00, 106.15 (C-3, 6), 126.32, 126/44, 126.48, 126.86, 127.03, 127.13, 128.97, 129.28, 129.42 (-ArH), 131.98, 132.88, 133.41 (C-1'' and –Ar-C), 155.04, 161.95, 163.32, 166.16 (C-2, 5, 7, 9), 182.64 (-C=O).

*4.5.2.9 5, 7-dihydroxy-6-((4-(2-hydroxyethyl)piperazin-1-yl)methyl)-2-(4-hydroxyphenyl) chroman-4-one (**17**)*

Yield: 64 %. White solid. ^{1}H NMR (400 MHz, MeOD-d_4): δ 2.56- 2.59 (2H, -NCH_2-, t, J = 5.8 Hz), 2.66-2.71 (5H, -N-CH_2-CH_2-N- and H-3, br), 2.90 (4H, -N-CH_2-CH_2-N-, br), 3.03 -3.10 (1H, H-3, dd, J = 12.6, 17.1 Hz), 3.67-3.70 (2H, -CH_2-OH, t, J = 5.8 Hz), 3.92 (2H, H-1'', s), 5.29 (1H, H-2, dd, J = 3.1, 12.6 Hz), 5.82 (1H, H-8, s), 6.82-6.84 (2H, H -3', 5', d, J = 8.56 Hz), 7.30-7.32 (2H, H-2', 6', d, J = 8.56 Hz); ^{13}C NMR (100 MHz, MeOD-d_4): 43.84 (C-3), 52.65 (C-1''), 52.84 and 53.22 (-N-CH_2-CH_2-N-), 59.89 (-N-

CH_2-), 60.79 (-CH_2-OH), 80.19 (C-2), 97.73 (C-8), 100.94 (C-10), 101.63 (C-6), 116.35 (C-3', 5'), 128.98 (C-2', 6'), 131.31 (C-1'), 158.97, 163.50, 164.43 (C-5, 9, 4'), 173.55 (C-7), 196.70 (C-4).

*4.5.2.10 5, 7-dihydroxy-6-((4-(2-hydroxyethyl)piperazin-1-yl)methyl)-2-phenyl-4H-chromen-4-one (**18**)*

Yield: 45 %. Yellow solid. ^{1}H NMR (400 MHz, $CDCl_3$): δ 2.57-2.61 (10H, 5 × -CH_2-N-), 3.64 (2H, -OCH_2-), 3.88 (2H, Ar-CH_2-N-), 6.41 (1H, H-8), 6.63 (1H, H-3), 7.52 (3H, H-3', 4', 5'), 7.87 (2H, H-2', 6'); ^{13}C NMR (100 MHz, DMSO-d_6): δ 52.58, 53.27 (-NCH_2CH_2N-), 53.88 (C-1''), 57.98 (-OCH_2-), 59.26 (-CH_2-N-), 94.69 (C-8), 103.58 (C-10), 104.42 (C-6), 105.69 (C-3), 126.38 (C-2', 6'), 129.17 (C-3', 5'), 131.57 (C-4'), 131.82 (C-1'), 157.36 (C-9), 159.35 (C-5), 163.82 (C-2), 165.97 (C-7), 182.53 (C=O).

*4.5.2.11 5, 7-dihydroxy-8-((4-(2-hydroxyethyl)piperazin-1-yl)methyl)-2-phenyl-4H-chromen-4-one (**19**)*

Yield: 55 %. Yellow solid. ^{1}H NMR (400 MHz, $CDCl_3$): δ 2.589-2.62 (10H, 5 × -CH_2-N-), 3.64 (2H, -OCH_2-), 4.02 (2H, Ar-CH_2-N-), 6.30 (1H, H-6), 6.64 (1H, H-3), 7.56 (3H, H-3', 4', 5'), 7.82 (2H, H-2', 6'); ^{13}C NMR (100 MHz, $CDCl_3$): δ 52.87, 52.68 (-NCH_2CH_2N-), 53.88 (C-1''), 57.97 (-OCH_2-), 59.17 (-CH_2-N-), 98.46, 100.43, 104.94, 106.05 (C-6, 10, 8, 3), 126.23 (C-2', 6'), 129.35 (C-3', 5'), 131.73 (C-4'), 131.95 (C-1'), 154.91 (C-9), 161.83 (C-5), 163.27 (C-2), 165.74 (C-7), 182.54 (C=O).

*4.5.2.12 Ethyl-4-((5, 7-dihydroxy-23-(4-hydroxyphenyl)-4-oxochroman-6-yl)methyl) piperazine-1-carboxylate (**20**)*

Yield: 64 %. White solid. ^{1}H NMR (400 MHz, MeOD-d_4): δ 1.13-1.18 (3H, m, -CH_3), 2.52 (4H, br, -N-CH_2-CH_2-N-), 2.58-2.63 (1H, H-3, dd, J = 3.0, 17.1 Hz), 2.96- 3.04 (1H, H-3, dd, J = 12.7, 17.1 Hz), 3.44 (4H, br, -N-CH_2-CH_2-N-), 3.67 (2H, s, H-1''), 4.02 (2H, m, -OCH_2-) 5.21-5.28 (1H, H-2, dd, J = 3.0, 12.7 Hz), 5.80 (1H, H-8, s), 6.70-6.72 (2H, H-3', 5', d, J = 8.6 Hz), 7.19-7.21 (2H, H-2', 6', d, J = 8.6 Hz); ^{13}C NMR (100 MHz, MeOD-d_4): 14.89 (-CH_3), 43.95 (C-3), 44.34 (-N-CH_2-CH_2-N-), 52.51 (C-1''), 53.12 (-N-CH_2-CH_2-N-), 62.89 (-OCH_2-), 80.44 (C-2), 96.61 (C-8), 101.96 (C-6), 116.36 (C-3', 5'), 129.02 (C-2', 6'), 131.19 (C-1''), 157.5, 159.05, 163.15, 164.20 (C-5, 7, 9, 4'), 169.65 (-N-C=O), 197.74 (-C=O).

*4.5.2.13 Ethyl-4-((5,7-dihydroxy-4-oxo-2-phenyl-4H-chromen-6-yl)methyl)piperazine-1-carboxylate (**21**)*

Yield: 50 %. Yellow solid. ^{1}H NMR (400 MHz, DMSO-d_6): δ 1.27 (3H, -CH_3), 2.61 (4H, H-3'', 7''), 3.5 (4H, H-4'', 6''), 4.01 (2H, H-1''), 4.14 (2H, -OCH_2-), 6.30 (1H, H-8), 6.64 (1H, H-3), 7.53 (3H, H-3', 4', 5'), 7.80 (2H, H-2', 6'); ^{13}C NMR (100 MHz, DMSO-d_6): δ 14.77 (-CH_3), 43.52 (C-4'', 6''), 52.55 (C-1''), 53.97 (C-3'', 7''), 61.82 (-OCH_2-), 98.23 (C-8), 100.45 (C-10), 105.03 (C-3), 106.09 (C-6), 126.21, 129.35, 131.66, 131.96 (C-2', 3', 4', 1'), 154.94 (C-9), 155.36 (-OC=O), 161.94, 163.29, 165.38 (C-2, 5, 7), 182.51 (-C=O).

*4.5.2.14 Diethyl-4, 4'-((5,7-dihydroxy-4-oxo-2-phenyl-4H-chromene-6,8-diyl)bis(methylene))bis(piperazine-1-carboxylate) (**22**)*

Yield: 37 %. Yellow solid. ^{1}H NMR (400 MHz, $CDCl_3$): δ 1.28 (6H, m, 2 × -CH_3), 2.62 (4H, br, H-3'', 7''), 3.56 (4H, br, H-4'', 6''), 3.87 (4H, 2 × s, H-1''), 4.14 (4H, m, 2 × -

OCH_2-), 6.67 (1H, s, H-3), 7.55 (3H, H-3', 4', 5'), 7.87 (2H, H-2', 6'); ^{13}C NMR (100 MHz, $CDCl_3$): representative peaks: δ 14.52 (-CH_3), 43.09, 43.31 (C-4'', 6''), 51.63, 52.04 (C-1''), 54.87 (C-3'', 7''), 60.65, 60.74 (-OCH_2-), 101.35, 102.53, 104.54, 104.8 (C-6, 8, 10, 3), 126.27, 129.19, 131.04, 131.87 (C-2', 3', 4', 1'), 154.50 (C-9), 154.69 (-OC=O), 181.68 (-C=O).

*4.5.2.15 Ethyl 4-(4-((5, 7-dihydroxy-2-(4-hydroxyphenyl)-4-oxochroman-6-yl)methyl) piperazin-1-yl)benzoate (**23**)*

Yield: 76%, white solid. ^1H NMR (400 MHz, $CDCl_3$): δ 1.22 (3H, t, -CH_3), 2.62 (1H, dd, J = 3.0, 17.1 Hz, H-3), 2.92 (1H, dd, J = 12.8, 17.1 Hz, H-3), 2.60- 3.36 (8H, br, 2 × -N-CH_2-CH_2-N-) 3.69 (2H, s, -N-C**H$_2$**-Ar), 4.20 (2H, q, -C**H$_2$**-CH_3), 5.20 (1H, dd, J = 3.0, 12.8 Hz, H-2), 5.83 (1H, s, H-8), 6.72 (4H, two doublets, J_1 = 8.5 Hz, J_2 = 8.8 Hz, -ArH), 7.17 (2H, d, J = 8.5 Hz, -ArH), 7.78 (2H, d, J = 8.8 Hz, -ArH); ^{13}C NMR (100 MHz, $CDCl_3$): 14.39 (-CH_3), 43.13 (C-3), 47.58 (C-1''), 52.12, 53.01 (-N-**C**H_2-**C**H_2-N-), 60.45 (-O-CH_2), 78.76 (C-2), 96.01 (C-8), 100.13 (C-10), 102.10 (C-6), 114.14 (-Ar), 115.65 (C-3', 5'), 121.05 (-C-C=O), 127.89 (C-2', 6'), 131.20 (-Ar), 137.67 (-Ar-N-), 153.67 (C-4'), 156.12 (C-9), 161.34 (C-5), 166.57 (C-7), 168.17 (-O-C=O), 195.78 (-C=O).

Acknowledgements

We thank the New Jersey Agricultural Experiment Station, and NIFA Hatch Project 1005685 and NJ12158, the School of Environmental and Biological Sciences at Rutgers and the New Use Agriculture and National Plant Products Program for partial funding and support. This work was conducted as part of the dissertation research of Jing Zhen.

5. References

[1] IDF Diabetes Atlas, 6th edn. 2014 update. Brussels, Belgium: International Diabetes Federation, International Diabetes Federation2014.

[2] L. Guariguata, D. Whiting, I. Hambleton, J. Beagley, U. Linnenkamp, J. Shaw, Global estimates of diabetes prevalence for 2013 and projections for 2035, Diabetes research and clinical practice, 103 (2014) 137-149.

[3] R. Tundis, M. Loizzo, F. Menichini, Natural products as α-amylase and α-glucosidase inhibitors and their hypoglycaemic potential in the treatment of diabetes: an update, Mini reviews in medicinal chemistry, 10 (2010) 315-331.

[4] R. Pili, J. Chang, R.A. Partis, R.A. Mueller, F.J. Chrest, A. Passaniti, The α-glucosidase I inhibitor castanospermine alters endothelial cell glycosylation, prevents angiogenesis, and inhibits tumor growth, Cancer research, 55 (1995) 2920-2926.

[5] A. Mehta, N. Zitzmann, P.M. Rudd, T.M. Block, R.A. Dwek, α-Glucosidase inhibitors as potential broad based anti-viral agents, FEBS letters, 430 (1998) 17-22.

[6] A.J. Scheen, Is there a role for α-glucosidase inhibitors in the prevention of type 2 diabetes mellitus?, Drugs, 63 (2003) 933-951.

[7] P. Hollander, Safety profile of acarbose, an α-glucosidase inhibitor, Drugs, 44 (1992) 47-53.

[8] M. Iio, A. Yoshioka, Y. Imayoshi, C. Koriyama, M. Ayako, Effect of flavonoids on α-glucosidase and β-fructosidase from yeast, Agr Biol Chem Tokyo, 48 (1984) 1559-1563.

[9] G.G. Wang, X.H. Lu, W. Li, X. Zhao, C. Zhang, Protective effects of luteolin on diabetic nephropathy in STZ-induced diabetic rats, Evid-Based Compl Alt, 2011 (2011).

[10] T.R. Helgren, R.J. Sciotti, P. Lee, S. Duffy, V.M. Avery, O. Igbinoba, M. Akoto, T.J. Hagen, The synthesis, antimalarial activity and CoMFA analysis of novel aminoalkylated quercetin analogs, Bioorg Med Chem Lett, 25 (2015) 327-332.

[11] H.T. Li, F. Zhu, H.Y. Chen, K.W. Cheng, T. Zykova, N. Oi, R.A. Lubet, A.M. Bode, M.F. Wang, Z.G. Dong, 6-C-(E-phenylethenyl)-Naringenin Suppresses Colorectal Cancer Growth by Inhibiting Cyclooxygenase-1, Cancer research, 74 (2014) 243-252.

[12] S. Khadem, R.J. Marles, Chromone and flavonoid alkaloids: occurrence and bioactivity, Molecules, 17 (2011) 191-206.

[13] H.H. Sedlacek, Mechanisms of action of flavopiridol, Critical reviews in oncology/hematology, 38 (2001) 139-170.

[14] F. Brindis, R. Rodríguez, R. Bye, M.n. González-Andrade, R. Mata, (Z)-3-Butylidenephthalide from Ligusticum porteri, an α-Glucosidase Inhibitor, J Nat Prod, 74 (2010) 314-320.

[15] L. Chen, T.S. Hu, J. Zhu, H.M. Wu, Z.J. Yao, Application of a regioselective Mannich reaction on naringenin and its use in fluorescent labeling, Synlett, (2006) 1225-1229.

[16] T.B. Nguyen, Q. Wang, F. Gueritte, An Efficient One-Step Synthesis of Piperidin-2-yl and Pyrrolidin-2-yl Flavonoid Alkaloids through Phenolic Mannich Reactions, Eur J Org Chem, (2011) 7076-7079.

[17] A. Cornish-Bowden, A simple graphical method for determining the inhibition constants of mixed, uncompetitive and non-competitive inhibitors, Biochemical Journal, 137 (1974) 143.

[18] T. Wang, X. Li, B. Zhou, H. Li, J. Zeng, W. Gao, Anti-diabetic activity in type 2 diabetic mice and α-glucosidase inhibitory, antioxidant and anti-inflammatory potential

of chemically profiled pear peel and pulp extracts (Pyrus spp.), J Funct Foods, 13 (2015) 276-288.

[19] L. Zhang, C.-S. Jiang, L.-X. Gao, J.-X. Gong, Z.-H. Wang, J.-Y. Li, J. Li, X.-W. Li, Y.W. Guo, Design, synthesis and in vitro activity of phidianidine B derivatives as novel PTP1B inhibitors with specific selectivity, Bioorg Med Chem Lett, 26 (2016) 778-781.

[20] O. Trott, A.J. Olson, AutoDock Vina: improving the speed and accuracy of docking with a new scoring function, efficient optimization, and multithreading, Journal of computational chemistry, 31 (2010) 455-461.

[21] W.L. DeLano, The PyMOL molecular graphics system, (2002).

[22] S. Nakamura, K. Takahira, G. Tanabe, T. Morikawa, M. Sakano, K. Ninomiya, M. Yoshikawa, O. Muraoka, I. Nakanishi, Docking and SAR studies of salacinol derivatives as α-glucosidase inhibitors, Bioorg Med Chem Lett, 20 (2010) 4420-4423.

Graphical abstract

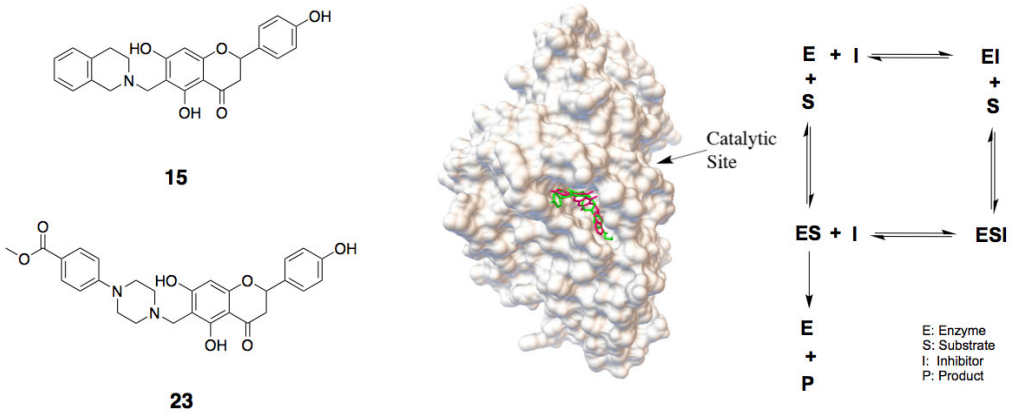

Highlights

- Novel synthesized synthetic flavonoid alkaloids could inhibit α-glucosidase
- Two compounds inhibit the enzyme in a non-competitive model
- SAR study reveals 4'-hyroxyl group and the 4-position carbonyl group are important.